Bathochromically shifted polymethine dyes through silicon incorporation

Monica Pengshung,[†] Junho Kwon[†] and Ellen M. Sletten*[,†]

[†]Department of Chemistry and Biochemistry, University of California, Los Angeles, 607 Charles E. Young, Dr. E., Los Angeles, CA 90095, USA.

ABSTRACT: Methods to red-shift fluorophores have garnered considerable interest due to the broad utility of low energy light. The incorporation of silicon into xanthene scaffolds has resulted in an array of visible and near-infrared fluorophores. Here, we extend this approach to polymethine dyes, another popular fluorophore class. We found that when oxygen was replaced with $SiMe_2$, bathochromic shifts of up to 121 nm and fluorophores with emission above 900 nm were achieved.

Fluorescence is a vital research tool for analysing molecules in complex, dilute environments. Using fluorescence microscopy, multiple molecular processes can be visualized simultaneously in real time at low concentrations.[1] Key to the success of fluorescent analyses are fluorophores. Over the past few centuries, thousands of small molecule chromophores have been prepared for the visible (VIS, 350–700 nm) region of the electromagnetic spectrum. Classic fluorophore scaffolds include polycyclic aromatic hydrocarbon, coumarin, fluorescein, rhodamine, and cyanine dyes.[1] Collectively, these fluorophores have enabled fundamental materials and biological studies; however, due to limitations of light penetration through heterogeneous materials there has been interest in red-shifting fluorophores to the near-infrared (NIR, 700–1000 nm) region and beyond.[2,3]

In 2008, Xu and coworkers reported that the introduction of silicon into a xanthene chromophore in place of oxygen resulted in a bathochromic shift of 100 nm (Figure 1A).[4] The red-shift imparted by silicon has been attributed to a low-lying LUMO arising from mixing of the σ* orbital of the silylene moiety with the π* orbital of the heterocycle.[5] Following this initial work, the use of silicon to red-shift fluorophores has been applied to oxazine, fluorescein and rhodamine dyes (Figure 1B, C, D).[6–10] These silicon-containing fluorophroes have been shown to be bright probes with advantageous photostability. We now extend silicon incorporation to another ubiquitous class of fluorophores, polymethine dyes, for the first time.

Polymethine dyes are known for their narrow absorption bands, high absorption coefficients, and readily tunable λ_{max} within the visible and near-infrared regions. These qualities lead to broad applications such as multiplexed imaging, Forster resonance energy transfer probes, microarray analyses, and light harvesting.[11–15] The most common polymethines are cyanine dyes, which have nitrogen-containing heterocycles connected via a polymethine chain (Figure 1E). A widely utilized approach to significantly modulate the λ_{max} of cyanine dyes is to vary the length of the polymethine chain, which leads to ~100 nm red-shift for each additional vinylene unit.[11] However, as the polymethine chain is extended the stability of the dye is decreased.[17] An alternative strategy to afford large red-shifts is diverging from the cyanine scaffold and replacing the nitrogen with a different heteroatom. This approach has yielded polymethine dyes containing O, S, Se, and Te but surprisingly not Si despite its popularity in other fluorophore scaffolds.[18] Herein, we demonstrate that the incorporation of silicon into heterocycles for polymethine dyes can impart red-shifts of similar magnitude to extension of the polymethine chain, while also enhancing photostability, resulting in fluorophores with emission above 900 nm (Figure 1F).

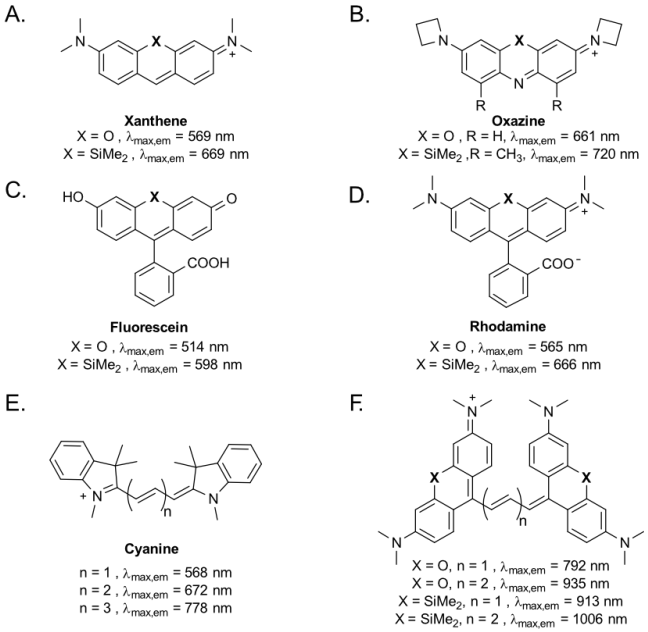

Figure 1. Fluorophore scaffolds. A) Xanthene scaffold, the first fluorophore where silicon was incorporated.[4] B) Oxazine scaffold.[9] C) Fluorescein scaffold.[10] D) Rhodamine scaffold.[10] E) Cyanine scaffold: a classic polymethine dye.[11] F) This work on silicon polymethines and their oxygen counterparts.[16]

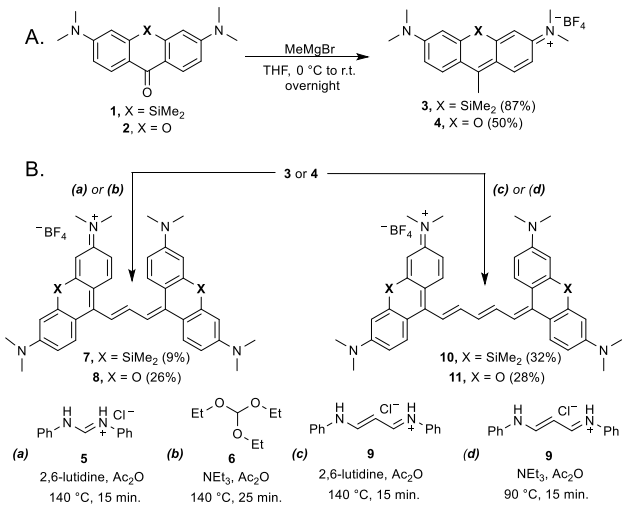

Scheme 1. Synthesis of silicon and oxygen fluorophores studied herein. A) Methyl Grignard addition into xanthone (**1** or **2**) afford xanthene-based silicon and oxygen heterocycles, **3** and **4** respectively. B) Refluxing heterocycle **3** or **4** with base and appropriate linker in acetic anhydride afforded silicon and oxygen polymethines. For **7**, conditions **(a)**. For **8**, conditions **(b)**. For **10**, conditions **(c)**. For **11**, conditions **(d)**.

To prepare polymethine fluorophores, heterocycles that can readily react with electrophilic polyene linkers are necessary. We envisioned that a suitable silicon-containing heterocycle could be prepared by methyl Grignard addition into known silicon xanthone **1**. We prepared **1** according to literature procedures[19] and treated it with MeMgBr to yield **3** in 87% yield (Scheme 1A). Silicon xanthylium **3** proved to be a bright, new, fluorophore with $\lambda_{max,abs}$ = 646 nm and $\lambda_{max,ems}$ = 673 nm (Figure 2, blue). Notably, this is 100 nm red-shifted from the oxygen congener **4**, which we synthesized as a control (Scheme 1A). The red-shifted photophysical properties of the heterocycle were promising for the development of bathochromically shifted polymethine fluorophores.

To synthesize the first generation of silicon polymethines, **3** was deprotonated with 2,6-lutidine and combined with diphenylformamidinine (**5**) in acetic anhydride (Scheme 1B) to afford **7** as a dark blue solid. Trimethine **7** displayed an absorption band that ranged from 550 to 950 nm with $\lambda_{max,abs}$ at 854 nm and $\lambda_{max,ems}$ at 913 nm (Figure 2, red). Additionally, we prepared the pentamethine dye **10** through a similar procedure substituting diphenylformamidinine with malonaldehyde bis(phenylimine) monohydrochloride (**9**) to yield **10** (Scheme 1B). Pentamethine **10** had a similar absorption band to **7** extending from 550 nm to 1000 nm with a $\lambda_{max,abs}$ at 938 nm and $\lambda_{max,ems}$ at 1006 nm (Figure 2, black).

The absorbance spectra of silicon polymethines **7** and **10** extended over hundreds of nanometers and contained two distinct peaks (Figure 2A), uncharacteristic of traditional cyanine dyes. The narrow absorbance of cyanine dyes arises from complete electron delocalization within the highest occupied molecular orbital (Figure 3A).[20] Broad absorption

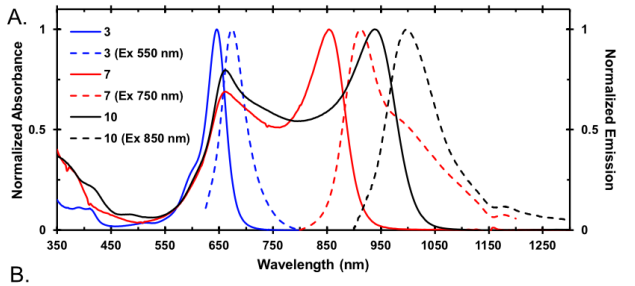

B.

Compound	$\lambda_{max,abs}$ (nm)	$\lambda_{max,ems}$ (nm)	ε (10^4, M^{-1} cm^{-1})	Φ_f (%)
3	646	673	3.5 ± 0.4	61 ± 5
7	854	913	3.9 ± 0.4	0.26 ± .02
10	938	1006	5.9 ± .02	0.19 ± .01

Figure 2. Photophysical data of silicon fluorophores. A) Normalized absorbance (solid) and emission (dotted) in dichloromethane. B) Photophysical characterization of **3, 7, 10** in dichloromethane.

spectra has been observed in long chain polymethines (>7 carbon units) and attributed to ground state desymmetrization.[20,21] Shorter chain polymethine dyes containing xanthene heterocycles have also been reported to display ground state destabilization, resulting in bimodal absorption spectra.[22] Upon ground state desymmetrization, electron delocalization within the polymethine is compromised such that asymmetric electronic configurations and dipolar character are observed (Figure 3B). Polar environments promote ground state destabilization due to their ability to stabilize localized partial charge.[23]

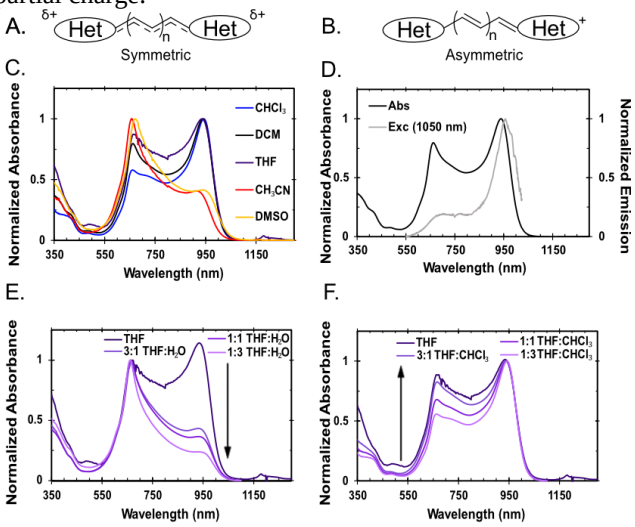

Figure 3. Photophysical data showing ground state desymmetrization of **10.** A) Schematic of symmetric state (delocalized) resembles a traditional polymethine fluorophore with partial positive character. B) Schematic of asymmetric state (dipolar) where charge is localized on one heterocycle. C) Absorbance of **10** (normalized to λ_{max}) in a range of nonpolar and polar solvents. D) Normalized absorption spectra (black) of **10** in dichloromethane. Normalized excitation spectra (grey) of **10**, with excitation from 515-1025 nm and collection 1050 nm in dichloromethane. E) Absorption spectra of **10** normalized at 663 nm in a solution of THF (0.01 mM) supplemented with increasing amounts of H_2O. F) Absorption spectra of **10** normalized at 938 nm in a solution of THF (0.01 mM) supplemented with increasing amounts of $CHCl_3$.

To investigate if ground state desymmetrization was responsible for the absorbance features of silicon-containing xanthene polymethine dyes, we performed solvatochromism studies.[24,25] The absorbance spectra of pentamethine **10** in dichloromethane has two distinct peaks at 663 nm and 938 nm in a 1 to 1.5 ratio, which we hypothesized to be due to the asymmetric and symmetric states, respectively (Figure 3C, black). A solvatochromism study revealed that the ratio of these peaks changed drastically with solvent polarity (Figure 3C), with polar solvents such as dimethyl sulfoxide (yellow, Figure 3C) and acetonitrile (red, Figure 3C) resulting in the 633 nm peak dominating (2.5 to 1). These results are consistent with previous findings that polar environments are able to stabilize the asymmetric state.[26] To more systematically study the effect of solvent polarity, we supplemented tetrahydrofuran containing **10** with more polar water or less polar chloroform (Figures 3D & 3E, respectively). These data are consistent with the solvatochromism studies and show opposite trends when increasing amounts of polar (water) or non-polar (chloroform) solvent are added. Analogous studies on trimethine **7** showed similar trends (Figure S1). Interestingly, the $\lambda_{max,abs}$ of the asymmetric state trimethine **7** is similar to pentamethine **10**, while their symmetric states differ by 84 nm. We attribute this to the asymmetric state having significant heterocycle character.

While the absorption of the silicon-containing polymethine dyes was broad and bimodal, the emission was well-defined with $\lambda_{max,ems}$ = 913 nm for **7** and 1006 nm for **10** (Figure 2A). The fluorescence quantum yields were characterized to be 0.26% ± 0.02% for **7** and 0.19% ± 0.01% for **10** in dichloromethane, relative to Flav5 (5% ± 2%)[27] and IR-26 (0.05% ± 0.03%),[28] respectively. Note that quantum yields for fluorophores above 900 nm are often quite low due to the small energy gap between the ground state and excited state.[29] The narrow emission band that does not mirror the absorption spectra is attributed to emission solely from the symmetrical state.[23] Excitation spectra confirmed that the symmetric state is responsible for the emission and little contribution comes from the asymmetric state (Figure 3D, gray). Additionally, emission spectra of **10** in polar solvents display minimal changes in peak shape and $\lambda_{max,ems,}$ although decreased signal in polar solvents is apparent (Figure S2). Collectively, these data support that the emissive species is primarily the symmetric state.

To showcase the direct benefit of silicon incorporation into the polymethine scaffold, we prepared oxygen congeners **8** and **11** (Scheme 1B, Figure S3). In both cases, the silicon-containing polymethines showed significant bathochromic shifts compared to their oxygen analogues (Figure 4A & 4B). When preforming a comparative analysis of the absorbance spectra, we found that the degree of bathochromic shift decreased as the polymethine linker increased. The absorbance difference at $\lambda_{max,abs}$ for the

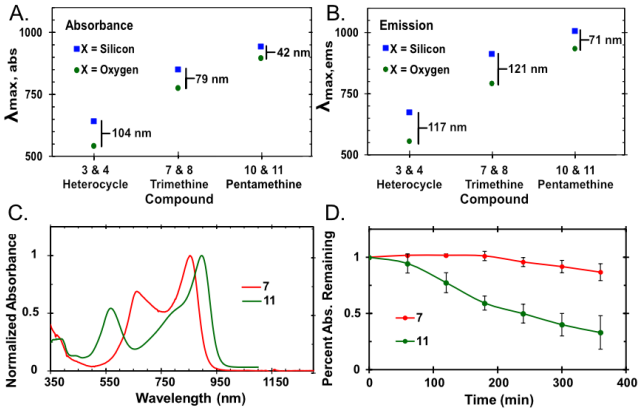

Figure 4. Comparison of silicon and oxygen xanthene polymethines. A/B) λ_{max} of silicon- (blue square) and oxygen- (green circle) containing polymethine fluorophores in dichloromethane. The values depicted on the plot indicate the degree of red-shift imparted by silicon. A) Absorbance. B) Emission. C) Normalized absorbance spectra of **7** and **11** in dichloromethane. D) Percent absorbance remaining at $\lambda_{max,abs}$ of **7** and **11** with continuous irradiation at 730 nm (146 mW/cm^2) over six hours. Error was taken as the standard deviation of three replicate experiments.

trimethines was 79 nm while the pentamethines was only 42 nm (Figure 5A). The degree of red-shift in the emission spectra was larger with a difference of 121 nm for the trimethines and 71 nm for the pentamethines (Figure 4B). The smaller shifts in absorbance are likely due to contributions from the asymmetric state. From these data, we conclude that that the incorporation of silicon into polymethine fluorophores in place of oxygen results in bathochromic shifts of the symmetric state by 70–100 nm, on par with extension of the polymethine chain. These values are also consistent with previous reports of incorporation of silicon into other fluorophore scaffolds.[9,10]

Finally, another advantage commonly cited for the use of silicon fluorophores is an increased photostability.[6,9] We evaluated the photostability of the silicon fluorophores compared to their oxygen analogues, focusing on the pair that has the most similar absorption: trimethine **7** and pentamethine **11** (Figure 4C). Photobleaching of **7** and **11** was performed by continuous irradiation with a 730 nm LED (146 mW/cm^2). We found that **11** began photobleaching rapidly within the first hour while **7** was unchanged over three hours (Figure 4D). Upon calculation of the photobleaching rate constants, we were able to quantify silicon-containing polymethine **7** as three-fold more stable than **11** (Figure S5). Photobleaching of silicon pentamethine **10** under the same conditions showed a similar decrease as **7** (Figure S4), suggestive that silicon incorporation plays an important role in increasing the photostability of the fluorophore.

In summary, we have demonstrated that incorporation of silicon into polymethine dyes is a valid approach to red-shift this class of fluorophores and is on par with vinylene chain extension. We prepared tri- and pentamethines with xanthene-derived hetereocycles which were 70–100 nm red-

shifted compared to oxygen analogues, resulting in emission at 913 nm and 1006 nm, respectively. The silicon-containing polymethines had advantageous photostability, three to twenty-fold more than their oxygen counterparts. The xanthene-derived heterocycles, while providing an efficient avenue for the synthesis of the first silicon polymethine dyes, also promoted ground state desymmetrization, which resulted in a broad, bimodal absorption spectrum and a decreased presence of the emissive species. Looking forward, the implementation of silicon into polymethine heterocycles that do not promote desymmetrization should provide avenues for the creation of deeply red-shifted (>900 nm) fluorophores with high photostability. Strategies for developing dyes within these regions of the electromagnetic spectrum are of significant interest to the materials and biomedical communities.

Acknowledgements

This work was supported by grants from the Sloan Research Award FG-2018-10855 and NIH 1R01EB027172-01, and instrumentation through the NSF MRI CHE-1048804 and NIH (1S10OD016387-01).

References

1 L. D. Lavis and R. T. Raines, *ACS Chem. Biol.*, 2008, 3, 142–155.

2 J. V Frangioni, *Curr. Opin. Chem. Biol.*, 2003, **7**, 626–634.

3 R. Weissleder, *Nat. Biotechnol.*, 2001, **19**, 316–317.

4 M. Fu, Y. Xiao, X. Qian, D. Zhao and Y. Xu, *Chem. Commun.*, 2008, 1780.

5 S. Yamaguchi and K. Tamao, *J. Chem. Soc. Dalt. Trans*, 1998, 3693–3702.

6 J. B. Grimm, T. A. Brown, A. N. Tkachuk and L. D. Lavis, *ACS Cent. Sci*, 2017, **3**, 975–985.

7 G. Lukinavičius, K. Umezawa, N. Olivier, A. Honigmann, G. Yang, T. Plass, V. Mueller, L. Reymond, I. R. Corrêa Jr, Z.-G. Luo, C. Schultz, E. A. Lemke, P. Heppenstall, C. Eggeling, S. Manley and K. Johnsson, *Nat. Chem.*, 2013, **5**, 132–139.

8 Y. Kushida, T. Nagano and K. Hanaoka, *Analyst*, 2015, 140, 685–695.

9 A. Choi and S. C. Miller, *Org. Lett.*, 2018, **20**, 4482–4485.

10 T. Ikeno, T. Nagano and K. Hanaoka, *Chem. - An Asian J.*, 2017, 12, 1435–1446.

11 J. L. Bricks, A. D. Kachkovskii, Y. L. Slominskii, A. O. Gerasov and S. V. Popov, *Dye. Pigment.*, 2015, **121**, 238–255.

12 M. Q. Doja, *Chem. Rev.*, 1932, **11**, 273–321.

13 H. A. Shindy, *Dye. Pigment.*, 2017, **145**, 505–513.

14 † Amaresh Mishra, Rajani K. Behera, Pradipta K. Behera, and Bijaya K. Mishra and G. B. Behera*, , DOI:10.1021/CR990402T.

15 S. Wang, Y. Fan, D. Li, C. Sun, Z. Lei, L. Lu, T. Wang and F. Zhang, *Nat. Commun.*, 2019, **10**, 1058.

16 M. P. Shandura, Y. M. Poronik and Y. P. Kovtun, *Dye. Pigment.*, 2005, **66**, 171–177.

17 A. V. Kulinich, A. A. Ishchenko, A. K. Chibisov and G. V. Zakharova, *J. Photochem. Photobiol. A Chem.*, 2014, **274**, 91–97.

18 M. R. Detty and B. J. Murray, *J. Org. Chem.*, 1982, **47**, 5235–5239.

19 T. Pastierik, P. Šebej, J. Medalová, P. Štacko and P. Klán, *J. Org. Chem.*, 2014, **79**, 3374–3382.

20 L. M. Tolbert and X. Zhao, *Beyond the Cyanine Limit: Peierls Distortion and Symmetry Collapse in a Polymethine Dye*, 1997.

21 L. M. Tolbert, *Solitons in a Box: The Organic Chemistry of Electrically Conducting Polyenes*, 1992, vol. 25.

22 S. V. Vasyluk, O. O. Viniychuk, Y. M. Poronik, Y. P. Kovtun, M. P. Shandura, V. M. Yashchuk and O. D. Kachkovsky, *J. Mol. Struct.*, 2011, **990**, 6–13.

23 F. Terenziani, O. V Przhonska, S. Webster, L. A. Padilha, Y. L. Slominsky, I. G. Davydenko, A. O. Gerasov, Y. P. Kovtun, M. P. Shandura, A. D. Kachkovski, D. J. Hagan, E. W. Van Stryland and A. Painelli, *J. Phys. Chem. Lett*, 2010, **1**, 1800–1804.

24 S. Webster, L. A. Padilha, H. Hu, O. V. Przhonska, D. J. Hagan, E. W. Van Stryland, M. V. Bondar, I. G. Davydenko, Y. L. Slominsky and A. D. Kachkovski, *J. Lumin.*, 2008, **128**, 1927–1936.

25 A. Yu, C. A. Tolbert, D. A. Farrow and D. M. Jonas, , DOI:10.1021/jp0205867.

26 H. Hu, O. V Przhonska, F. Terenziani, A. Painelli, D. Fishman, T. R. Ensley, M. Reichert, S. Webster, J. L. Bricks, A. D. Kachkovski, D. J. Hagan Ae and E. W. Van Stryland, *Phys. Chem. Chem. Phys*, 2013, **15**, 7666.

27 E. D. Cosco, J. R. Caram, O. T. Bruns, D. Franke, R. A. Day, E. P. Farr, M. G. Bawendi and E. M. Sletten, *Angew. Chemie Int. Ed.*, 2017, **56**, 13126–13129.

28 O. E. Semonin, J. C. Johnson, J. M. Luther, A. G. Midgett, A. J. Nozik and M. C. Beard, *J. Phys. Chem. Lett.*, 2010, **1**, 2445–2450.

29 E. Thimsen, B. Sadtler and M. Y. Berezin, *Nanophotonics*, 2017, **6**, 1043–1054.